

DESIGN & SIMULATION of a ROTATING APERTURE & VACUUM SYSTEM FOR NEUTRON IMAGING

Pete Fitsos (fitsos1@llnl.gov), James Hall (hall9@llnl.gov),
 Brian Rusnak(rusnak1@llnl.gov), Stewart Shen (shen2@llnl.gov)

Lawrence Livermore National Laboratory
 Livermore, California, 94550, USA

INTRODUCTION

The development of a high-energy (10MeV) neutron imaging system at Lawrence Livermore National Laboratory (LLNL) depends on a precision engineered rotating aperture and vacuum system for generating neutrons that are used for imaging dense objects. This subsystem is part of a larger system which includes a linear accelerator that creates a deuteron beam, a scintillator detector, imaging optics and a high resolution CCD camera.

A rotating aperture is a device that allows the high energy pulsed beam to interact with deuterium gas in a gas cell and thereby create the neutrons used for imaging (see Figures 1-3). The gas cell is flanked by two metal disks that rotate at 4000 rpm. The disks have two 5mm holes and act as a rotating aperture when the holes line up with holes in the gas cell and allow the deuteron beam to pass through into the gas cell. When the holes aren't lined up, gas from the gas cell leaks past the disks and into a vacuum vessel.

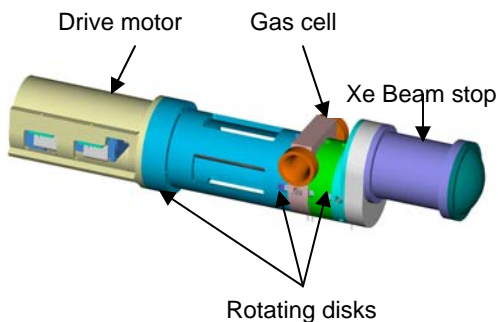


FIGURE 1. Rotating aperture assembly.

As the beam passes through the gas cell it interacts with deuterium gas flowing

perpendicular to the beam at 400 meter/sec and 3 atmospheres. This interaction creates a burst of neutrons that form a cone in the general direction of the beam. The remaining deuterons in the beam pass through another rotating aperture and into a gas cylinder filled with xenon

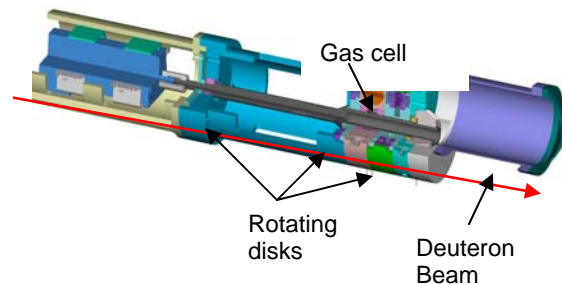


FIGURE 2. Cut away of rotating aperture assembly.

gas, which is able to stop the beam within 10 centimeters. This beam stop does not affect the cone of neutrons, which pass through and go on toward the object that is being imaged. The neutrons emerge from the object with different energies depending on geometry and density and collide with a scintillator, which converts the neutron energy into photons for imaging.

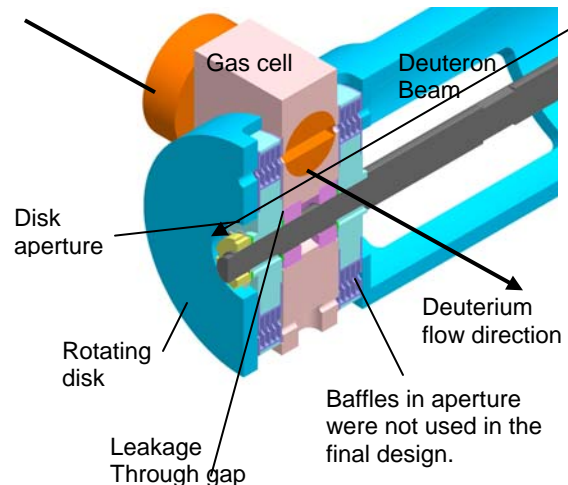


FIGURE 3. Detail of rotating disk and gas cell.

The entire rotating aperture system is enclosed in a vacuum vessel as shown in Figure 4 below.

Leakage of deuterium and xenon from the rotating apertures is pumped out of the vacuum vessel by scroll pumps sufficient to keep the pressure in the vessel at 10 Torr.

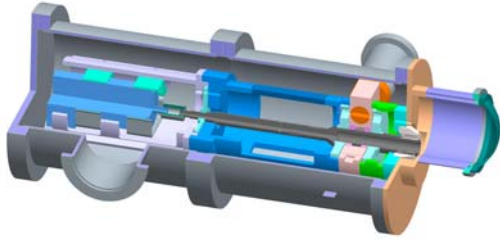


Figure 4. Cut away showing the rotating aperture system enclosed in a vacuum vessel.

SYSTEM MODELING

Modeling of the vacuum vessel, the rotating aperture leakages and the vacuum pumps was done by considering the total throughput of a pump, Q_{pump} and equating it to the change in pressure, P of a vessel, V and the various leakages into and out of the vessel, Q_{leakage} as shown below:

$$Q_{\text{pump}} = -V \left(\frac{dP}{dt} \right) + Q_{\text{leakage}} \quad (1)$$

Rearranging equation (1) and applying it to n number of vacuum vessels in the system leads to a system of coupled first order differential equations of the form:

$$\frac{dP_i}{dt} = (Q_{\text{leakages}})_i - (Q_{\text{pumps}})_i \quad \text{for } i=1..n \quad (2)$$

The throughput of the pumps, Q_{pump} was quantified using a pump function supplied by the manufacturer or derived by least square fit to the performance data supplied.

In our system the leakages, Q_{leakage} consisted of flows between vessels via conduits and leakages from the rotating aperture orifices. For leakage or flows between vessels the flows take

the form of the following equation as defined for vacuum systems [1]:

$$Q_{\text{leakage}} = C_{i,j} (P_i - P_j) \quad (3)$$

where $C_{i,j}$ = conductance between vessels i,j .

$P_{i,j}$ = pressure in vessels i,j .

Conductance is the proportional factor that relates the flow of molecules through a pipe cross section to the net molecular density or pressure difference across the pipe.

The leakage terms for the rotating aperture consisted of two terms: one for when the rotating aperture holes were not aligned and another for when the holes were aligned and there was subsonic or sonic flow through the aperture.

When the aperture holes are not aligned the flow is viscous and can be estimated by the following relationship for a long duct having an annular cross section between the tube r_o and that of the concentric core radius, r_i [1]:

$$C = \left(\frac{\pi}{8\eta} \right) \left(\frac{P_{\text{avg}}}{L} \right) \left[\left(r_o^4 - r_i^4 \right) - \frac{\left(r_o^2 - r_i^2 \right)^2}{\ln \left(\frac{r_o}{r_i} \right)} \right] \quad (4)$$

P_{avg} is the average pressure across the aperture, L is the length of the aperture and η the viscosity. For our application the difference in radii represents the gap between the rotating aperture disk and the stationary adjacent gas cell and is how the gas leaks into the vacuum vessel when the aperture is closed.

When the apertures are aligned the flow out of the gas cell and through the apertures becomes sonic or near sonic due to the much higher pressure in the gas cell. The mass flow rate through the aperture, \dot{m} is related to the gas density ρ , the speed of the gas c , and the area, A as follows [2]:

$$\dot{m} = \rho c A \quad (5)$$

Therefore the flow through aperture, Q is

$$Q = \frac{\dot{m}}{\rho} = c A \quad (6)$$

$$\text{and } c = \frac{c_0}{\sqrt{\frac{\gamma + 1}{2}}} \quad (7)$$

Where c_0 is the speed of sound for the gas and γ the ratio of specific heats.

The complete system model was programmed into Matlab with a first order differential equation of the form of equation (1) for each separate vessel. For the vessel that contained the rotating aperture, a routine in Matlab was used that would switch between the two leakage terms as a function of the rotating disk position. The complete model consisted of a series of coupled first order equations that was solved using Matlab integrators and yielded the pressure in each vessel as a function of time, vacuum pumps performance and leakages.

TEST RESULTS

Tests were conducted on an earlier version of the rotating aperture system enclosed in vacuum vessels as shown in Figure 5. For practical reasons helium gas was used in lieu of deuterium gas. The densities of the two gases are similar but helium is easier to come by and not flammable. A schematic of this test system is shown in Figure 6.

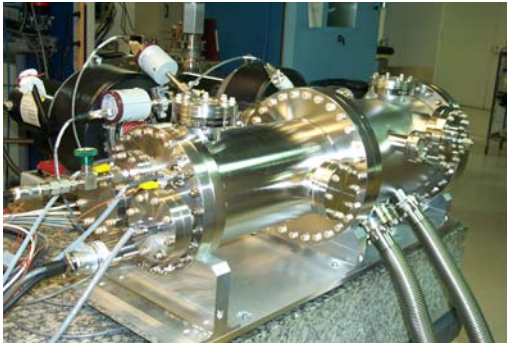


Figure 5. Earlier version of the rotating aperture

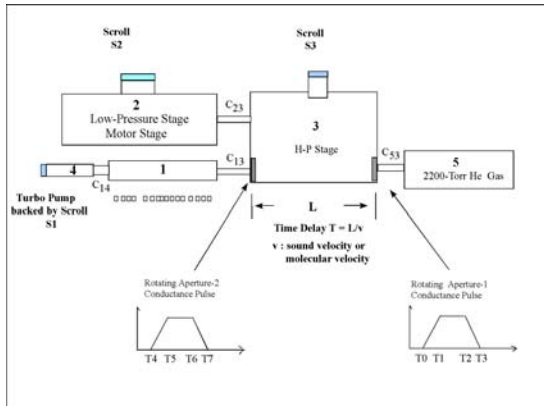


Figure 6. Schematic of rotating aperture, vacuum vessels and gas cell.

The model had 4 vessels and included 3 scroll pumps as used in the test setup. The gas cell pressure varied from 0 to 2200 Torr of helium. The state equations for each vessel of the system, is based on equation (2) above as follows (equations 8-11):

$$\frac{dP_1}{dt} = \frac{Q1 + G13[P_3 - P_1] + C14[P_4 - P_1]}{V1}$$

$$\frac{dP_2}{dt} = \frac{-[10.5e^{-.0015P_2}]P_2 + Q2 + C23[P_3 - P_2]}{V2}$$

$$\frac{dP_3}{dt} = \frac{Q3 - [10.5e^{-.0015P_3}]P_3 + C23[P_2 - P_3]}{V3} + \dots$$

$$\dots \frac{2 \cdot G35[2200 - P_3] + G13[P_1 + P_3]}{V3}$$

$$\frac{dP_4}{dt} = \frac{Q4 + C14[P_1 - P_4]}{V4}$$

Where

Q1-4 = out gassing in vessels 1 through 4.

G13=Aperture conductance between vessels 1 and 3.

G35=Aperture conductance between vessels 3 and 5.

C14= Conductance between vessels 1 and 4.

C23= Conductance between vessels 2 and 3.

$10.5e^{-.0015P_n}$ = Pump function for pump in vessel n.

$P_{1...4}$ = Pressure in vessels 1...4.

V1-4 = Volume of vessels 1 through 4.

For the tests the rotating aperture was driven to 1000 rpm and the gas cell pressure was varied as vacuum measurements were taken of vessel 3. The results showed a good correlation between measured and predicted as shown in Figure 7.

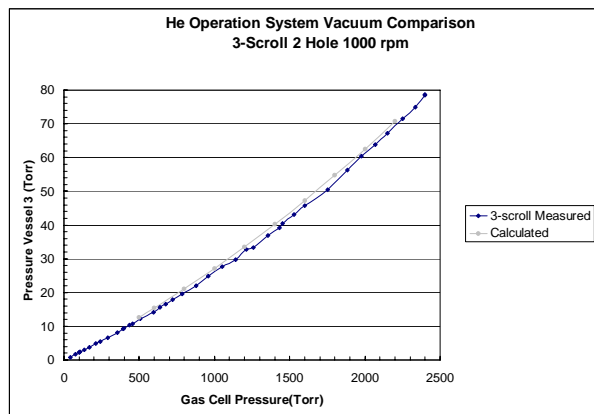


Figure 7. Pressure in vessel 3 vs. gas cell pressure for calculated and test results.

The increase in the pressure of vessel 3 with an increase in the gas cell pressure is due to the leakage from the rotating aperture. As the gas cell pressure increases so does the leakage into vessel 3. Figure 8 shows the composition of the gas leakage. Most of it comes from the pulse of gas that comes through the rotating aperture as the holes line up. A significant portion is the leakage that occurs when holes aren't linked up, This is controlled by the gap between the rotating disk and the adjacent gas cell well as shown in Figure 3.

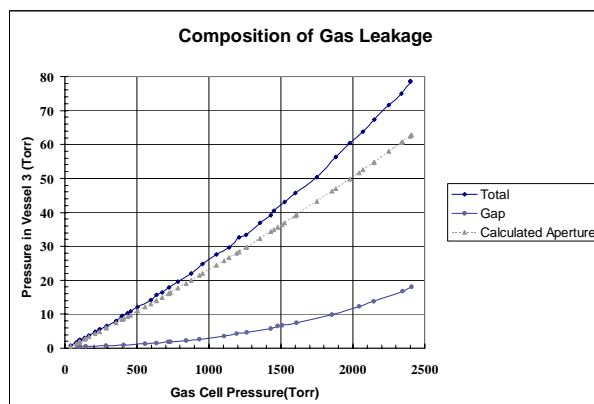


Figure 8. Composition of gas leakage. Pressure in vessel 3 vs. gas cell pressure.

The rotating aperture gap for the test setup was 68.5 microns. Simulations were done showing how this leakage, or conductance through the gap, relates to the gap spacing as shown in equation 4. Figure 9 shows how the leakage rate varies as a function of the gap and gas cell pressure.

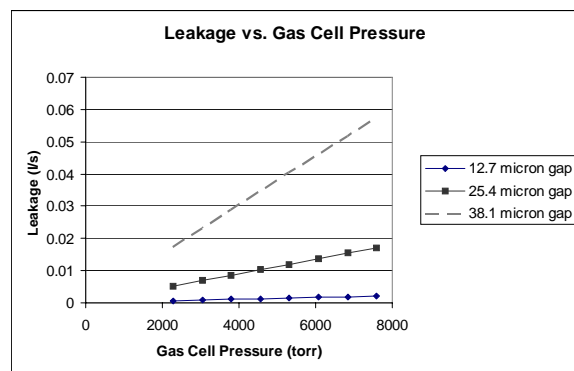


Figure 9. Simulation of rotating aperture leakage as a function of gas cell pressure and the gap.

Minimizing the gap depends on the run out of the bearings that support the shaft connecting the rotating disks. Using off the shelf bearings with a class 6 rating leads to a minimum practical gap of 12.7 microns. This spacing will be monitored during operation of the system using three capacitance gages on each side of the gas cell.

The main source of leakage into the vacuum vessel is due to gas flows into the vessel when the apertures are lined up (calculated aperture in Figure 8). It was thought that this gas flow could be reduced by using baffles in the aperture to provide an alternate path for the gas to flow and thereby reduce exit pressure. However simulations using the Computational Fluid Dynamics option in ANSYS showed no clear benefit and the final design will not include the baffles shown in Figure 3.

CONCLUSION

The rotating aperture vacuum system has been successfully simulated and tested. Results show the feasibility of the design and point toward ways to improve the design by minimizing the rotating aperture gap.

REFERENCES

1. Roth, A., 1998, *Vacuum Technology*, North-Holland, Amsterdam.
2. Thompson, P.A., 1972, *Compressible Fluid Dynamics*, McGraw-Hill New York.

This work was performed under the auspices of the U.S. Department of Energy by University of California, Lawrence Livermore National Laboratory under Contract W-7405-Eng-48.